

THERMAL DILEPTON RATES AND MESON SPECTRAL FUNCTIONS FROM LATTICE QCD

I. WETZORKE

NIC/DESY Zeuthen, Platanenallee 6, D-15738 Zeuthen, Germany

Abstract

Pseudo-scalar and vector meson correlation functions were calculated at temperatures below and above the deconfinement transition using $\mathcal{O}(a)$ improved Wilson fermions in quenched lattice QCD. The spectral functions were reconstructed from the correlator given only at discrete points in Euclidean time by means of the Maximum Entropy Method without a priori assumptions on the spectral shape. The deviation of the spectral functions from the one of a freely propagating quark anti-quark pair is examined above the critical temperature. At 1.5 and 3 T_c the vector spectral function yields an enhancement of the dilepton rate over the Born rate in the energy interval $4 < \omega/T < 8$ and a sharp drop at energies below 2-3 T.

1 Introduction

The thermal dilepton spectrum is accessible in heavy ion collisions and provides a key observable to study thermal properties of the medium at high density and temperature [1, 2]. Thermally induced changes of the dilepton spectrum at low energies [3] are expected to be influenced by non-perturbative in-medium modifications of the quark anti-quark interactions. Furthermore such effects are directly related to changes of the spectral shape in the vector meson channel. In two-flavor QCD the differential dilepton rate is connected to vector spectral function $\sigma_V(\omega, \vec{p}, T)$ through the relation

$$\frac{dN_{\bar{u}u}}{d^4x d^4p} \equiv \frac{dW}{d\omega d^3p} = \frac{5\alpha^2}{27\pi^2} \frac{1}{\omega^2 (e^{\omega/T} - 1)} \sigma_V(\omega, \vec{p}, T). \quad (1)$$

At the same time the spectral densities are related to the Euclidean correlation functions of hadronic currents $J_H(\tau, \vec{x}) = \bar{\psi}(\tau, \vec{x}) \Gamma_H \psi(\tau, \vec{x})$ with $\Gamma_H \in [1, \gamma_5, \gamma_\mu, \dots]$ through the integral equation

$$\begin{aligned} G_H(\tau, \vec{p}, T) &= \int d^3x e^{i\vec{p}\cdot\vec{x}} \langle J_H(\tau, \vec{x}) J_H^\dagger(0, \vec{0}) \rangle \\ &= \int_0^\infty d\omega \sigma_H(\omega, \vec{p}, T) \frac{\text{ch}(\omega(\tau - 1/2T))}{\text{sh}(\omega/2T)}. \end{aligned} \quad (2)$$

Although hadronic correlators can be calculated numerically in the framework of lattice regularized QCD for discrete Euclidean times $\tau \in [0, 1/T]$, the inversion of the integral equation still remains an ill-posed problem. This situation improved considerably after the implementation of the Maximum Entropy Method (MEM) for lattice QCD [4], which allows to obtain the most probable spectral function without a priori assumptions on the spectral shape.

Most of the previous applications of MEM concentrated on the analysis of hadronic properties like masses and decay width at zero temperature, where the pole masses of the ground [4, 5] and even excited states [6] could be obtained with quite satisfactory precision. The great challenge, however, is to apply the method at non-zero temperature, where very little about the spectral shape is known so far.

2 Thermal Meson Spectral Functions

At finite temperature excited states and continuum-like contributions are expected to gain in influence on the spectral shape. Thus it is mandatory to verify that the method allows to reconstruct such spectral functions correctly. A first step in this direction was the reconstruction of the spectral shape for free massless quarks in the (pseudo-)scalar channel $\sigma_{PS}^{free} = 3/8 \pi^{-2} \omega^2 \tanh(\omega/4T)$, known from leading order perturbation theory. In this case the relation (2) was used to obtain discrete values of the correlator in Euclidean time [5]. On the other hand such a correlator is directly calculable on the lattice [7], which is shown in figure 1(a) for three different lattice sizes. At small time separations the finite lattice cut-off effects are visible compared to the free continuum correlation function indicated as solid line. Nevertheless, the spectral shape could be reconstructed almost perfectly already for temporal extents $N_\tau = 8 \dots 16$ (see fig. 1(b)) by introducing a lattice version of the integration kernel in equation (2) for vanishing momentum

$$G_H(\tau, T) = \int_0^\infty d\omega \sigma_V(\omega, T) K_L(\tau, \omega, N_\tau) \quad , \quad (3)$$

where $K_L(\tau, \omega, N_\tau)$ is the finite lattice approximation of the continuum kernel

$$K_L(\tau, \omega, N_\tau) = \frac{2\omega}{T} \sum_{n=0}^{N_\tau-1} \frac{\exp(-i2\pi n\tau T)}{(2N_\tau \sin(n\pi/N_\tau))^2 + (\omega/T)^2} \quad . \quad (4)$$

Since the applicability of MEM at finite temperature has been verified, one can proceed to analyze meson spectral functions below and above the critical temperature of the deconfinement transition. We have calculated pseudo-scalar and vector meson correlation functions on large isotropic lattices of sizes

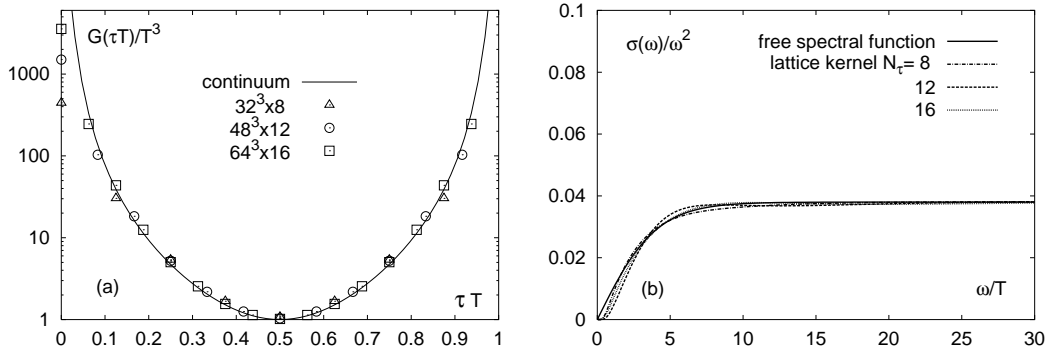


Figure 1: Free scalar correlators (a) and reconstructed spectral shape (b)

$(24 - 64)^3 \times 16$ in a temperature range 0.4 to $3.0 T_c$ using $\mathcal{O}(a)$ improved Wilson fermions [8] in quenched lattice QCD. Below T_c up to five quark mass values were chosen in order to obtain a reliable extrapolation to the chiral limit ($m_q \rightarrow 0$). Above the critical temperature the simulations could be performed directly at approximately zero quark mass, since there are no longer massless Goldstone modes present [9].

Compared to the sharp δ -function like peaks observed in the spectral functions at $T = 0$ [6] a broadening of the peaks corresponding to particle poles and a reduction in height can be observed at finite temperature. Figure 2 shows an example at $0.4 T_c$, where the error bars indicate the uncertainty in the given energy region calculated from the covariance matrix of the spectral function [10]. The ground state masses extracted from the spectral functions at $0.4 T_c$ agree very well with zero temperature data [11]. Increasing the temperature towards T_c the vector meson spectral function is investigated at fixed pion mass. The ground state peak experiences a further broadening and is slightly shifted towards higher energies. It remains to be clarified to what extent this effect is induced by the restricted temporal dimension and limited statistics.

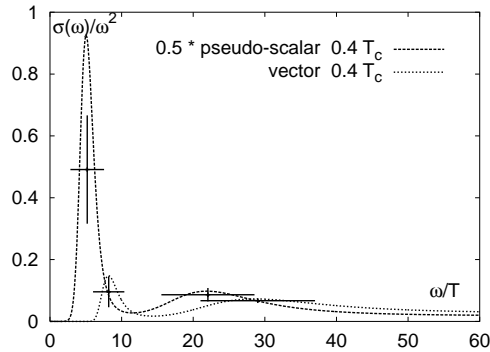


Figure 2: Meson spectral functions for a ratio of $m_\pi/m_\rho = 0.6$ at $0.4 T_c$

Above the critical temperature only a gradual approach towards the free correlation function is observed in the (pseudo-)scalar channel, while the vector

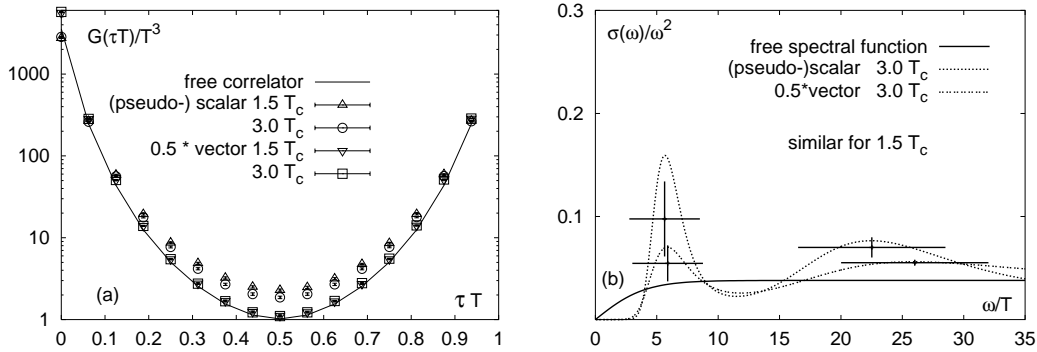


Figure 3: Meson correlators (a) and reconstructed spectral functions (b)

meson correlator is much closer to the free quark behavior already at $1.5 T_c$ (see fig. 3(a)). Analyzing directly the ratio of the correlation function in the vector channel to the corresponding free curve calculated for the same lattice size yields a deviation of about 10 %. The free correlator is approached from above, while simple quasi-particle pictures lead to a reduction of $G_V(\tau, T)$ relative to $G_V^{free}(\tau, T)$ [1, 12]. The deviations from the free quark behavior are also evident from the reconstructed spectral functions in figure 3(b). While the second enhancement over the free curve visible in fig. 2 and 3(b) at energies larger than $\omega/T = 16$ is presumably a lattice artifact due to the heavy fermion doublers of the Wilson fermion formulation [6], the peak at about $\omega/T = 6$ shows the actual physical effect of persisting interactions between quarks and gluons in both channels up to $3 T_c$. Compared to the zero temperature results [4, 5, 6] the peaks are rather broad and less pronounced in height, but might sharpen by increasing the statistics and the lattice size [4].

3 Thermal Dilepton Rates

Once the most probable vector meson spectral function is reconstructed from the correlation function in Euclidean times by means of the Maximum Entropy Method, the remaining step to obtain the differential dilepton rate is straight forward. The spectral functions shown in figure 4(a) were obtained from correlators on the largest lattice ($64^3 \times 16$) with approximately zero quark mass at temperatures 1.5 and $3.0 T_c$ [9]. In addition to the purely statistical error-band obtained from a Jackknife analysis, the uncertainty of the uniqueness of the result incorporated in MEM is shown in the insertion as error bars for four energy intervals. This leads to the conclusion that the data sample is large enough to yield statistically significant results.

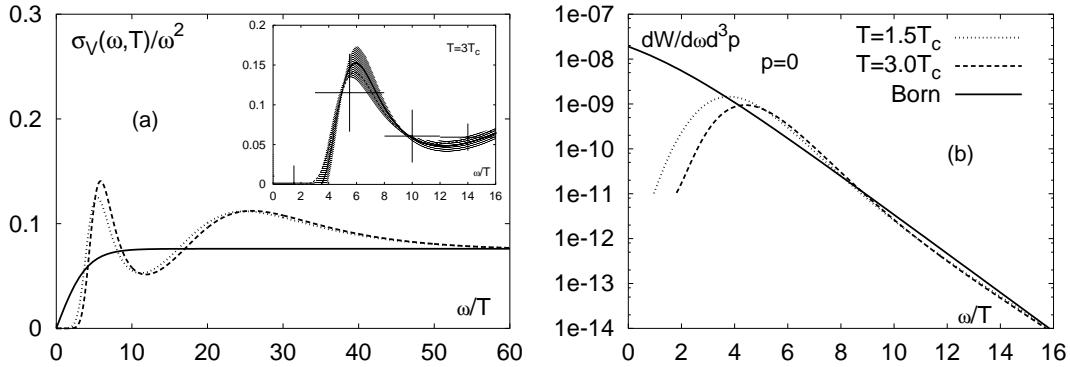


Figure 4: Vector spectral function (a) and differential dilepton rate (b)

The differential dilepton rate can now be calculated in employing relation (1) projected onto zero momentum. Figure 4(b) illustrates the corresponding dilepton rates for both temperatures. In the high temperature limit the leading order perturbative result can be obtained by using free massless quark propagators in the calculation of the current-current correlation functions. For vanishing momentum the spectral function in the vector channel is given by $\sigma_V^{free} = 3/4 \pi^{-2} \omega^2 \tanh(\omega/4T)$, which leads to the reduction of the differential dilepton rate to the Born rate

$$\frac{dW^{\text{Born}}}{d\omega d^3p}(\vec{p} = 0) = \frac{5\alpha^2}{36\pi^4} \frac{1}{(e^{\omega/2T} + 1)^2} \quad . \quad (5)$$

The broad peak visible in the spectral functions at around $\omega/T = 5 - 6$ results in an enhancement of the respective dilepton rates in the region $\omega/T = 4 - 8$ compared to the Born rate, which seems to scale with the temperature. For even larger energies the close agreement of the differential dilepton spectrum with the Born rate is evident.

The most striking feature of the observed dilepton rate is certainly the sharp drop at energies below $\omega/T = 2 - 3$. This effect is in contrast to hard thermal loop resummed perturbation theory [13] as well as to 2-loop perturbative calculations [14], which lead to a divergent vector spectral function in the limit $\omega \rightarrow 0$. If this suppressions persists in future investigations closer to the critical temperature, there would be no thermal contribution the dilepton rate at small energies during the expansion of the hot medium created in heavy ion collisions. This is consistent with the present results at SPS energies [15] and might be observable in the dilepton spectra at RHIC or LHC energies.

Acknowledgements

The work summarized in this talk is part of a very lively collaboration with F. Karsch, E. Laermann, P. Petreczky and S. Stickan. Furthermore, I want to thank the organizers of the Hirscheegg Workshop on Ultrarelativistic Heavy-Ion Collisions for the opportunity to present this contribution and many of the participants for fruitful discussions.

References

- [1] J. Kapusta, Phys. Lett. 136B (1984) 201
- [2] L.D. McLerran and T. Toimela, Phys. Rev. D31 (1985) 545;
J. Alam et al., Annals Phys. 286 (2001) 159
- [3] M.C. Abreu et al. (NA50), Phys. Lett. B450 (1999) 456
- [4] Y. Nakahara et al., Phys. Rev. D60 (1999) 091503;
M. Asakawa et al., Prog. Part. Nucl. Phys. 46 (2001) 459
- [5] I. Wetzorke and F. Karsch, in Proceedings of the International Workshop on Strong and Electroweak Matter 2000 (Edt. C.P. Korthals-Altes, World Scientific 2001), p.193, hep-lat/0008008
- [6] T. Yamazaki et al. (CP-PACS Coll.), Phys. Rev. D65 (2002) 014501
- [7] D.B. Carpenter and C.F. Baillie, Nucl. Phys. B260 (1985) 103
- [8] B. Sheikholeslami and R. Wohlert, Nucl. Phys. B259 (1985) 572;
M. Lüscher et al., Nucl. Phys. B491 (1997) 344
- [9] F. Karsch et al., hep-lat/0110208
- [10] R.K. Bryan, Eur. Biophys. J. 18 (1990) 165
- [11] M. Göckeler et al., Phys. Rev. D57 (1998) 5562
- [12] M.G. Mustafa et al., Phys. Rev. C61 (1999) 024902;
F. Karsch et al., Phys. Lett. B497 (2001) 249
- [13] E. Braaten et al., Phys. Rev. Lett. 64 (1990) 2242;
P. Aurenche et al., Phys. Rev. D58 (1998) 085003
- [14] T. Altherr and P. Aurenche, Z. Phys. C 45 (1989) 99
- [15] G. Agakichiev et al. (CERES Coll.), Phys. Lett. B422 (1998) 405